Molecular Modeling of the Reduction Mechanism in the Citrate-Mediated Synthesis of Gold Nanoparticles

Isaac Ojea-Jiménez[†] and Josep M. Campanera[‡],*

[†]Centre d'Investigació en Nanociència i Nanotecnologia (CIN2, ICN-CSIC), Campus UAB, 08193, Cerdanyola del Vallès, Spain
[‡]Departament de Fisicoquímica, Facultat de Farmàcia, Universitat de Barcelona, Av. Joan XXIII, s/n, Diagonal Sud, 08028 Barcelona, Spain

S *Supporting Information*

ABSTRACT: The synthesis of gold nanoparticles (Au NPs) via the reduction of tetrachloroauric acid by sodium citrate has become a standard procedure in nanotechnology. Simultaneously, gold-mediated reactions are gaining interest due to their catalytic properties, unseen in other metals. In this study, we have investigated the theoretical mechanism of this reaction under three different pH conditions (acid, mild acid, and neutral) and have corroborated our findings with experimental kinetic measurements by UV−vis absorption spectroscopy and transmission electron microscopy (TEM) analysis of the final particle morphology. We have demonstrated that, indeed, the pH of the medium ultimately determines the reaction rate of the reduction, which is the rate-limiting step in the Au NPs formation and involves decarboxylation of the citrate. The pH sets the dominant species of each of the reactants and, consequently, the reaction pathways slightly differ in each pH condition. The mechanism highlights the effect of the number of Cl$^-$ ligands in the metallocomplex, which ultimately originates the energetic differences in the reaction paths.
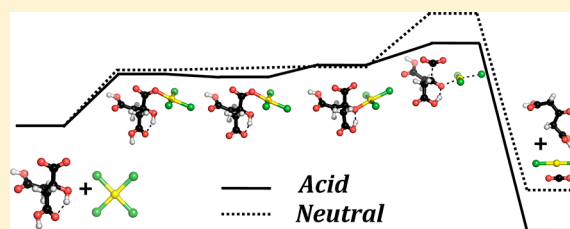
I. INTRODUCTION

Au NPs have become a standard reference material[1] as well as a fundamental tool for research in many fields of nano-technology.[2,3] While many recipes are available for the formation of uniform colloidal Au NPs, one of the most widely employed is still the classical reduction of tetrachloroauric acid in aqueous solution with sodium citrate, pioneered by Turkevich and co-workers in 1951.[4,5] Since then, many variants of this simple experimental protocol have been proposed such as changing the ratio of sodium citrate to gold salt,[6] controlling the reaction mixture pH,[7] reverting the sequence of reagents addition[8,9] or modifying the solvent.[10] These parameters affect the distribution of reactive species in solution, therefore altering the rates of reduction, nucleation and growth, and ultimately influencing the final particle size and size distribution.

A number of different models that attempt to explain the features of Au NP synthesis have been presented. For example, contrary to the classical Lamer nucleation−growth model,[11] Chow and Zukoski demonstrated that the initial period of nucleation favored the formation of large aggregates, resulting from the reduction of Au(III) by citrate, which fall apart during the course of the reaction to produce small monodisperse particles.[12] Further studies by Liz-Marzán and co-workers supported this reaction mechanism by electrochemical measurements, which showed drastic changes in particle charge and redox potential during the particle formation, and concluded that the reduction of Au(III) to Au(I) is the rate limiting step in both nucleation and growth phases.[13] Furthermore, as initially postulated by Turkevich and co-workers,[5] and later demonstrated by us,[8] the induction period prior to gold colloid nucleation is associated with the need to form citrate oxidation products, such as dicarboxyacetone, which acts as a multidentate quelating agent that produces clusters of Au(I). During this time, the concentration of Au(I) species increases to a level high enough (approximately to 10 nM [AuCl$_2$]$^-$) to trigger disproportionation and the sub-sequent supersaturation of Au(0) atoms in solution.[14]

The rate of reduction observed in the formation of Au NPs is a reflection of the conflicting trends in pH-dependent reactivity of citrate and auric species. Goia and Matijevic estimated the probable variation of the standard redox potential of the different Au(III) complexes and the reducing agent driven by the variations in pH of the initial reaction mixture.[15] On the basis of these studies, Peng and co-workers disclosed that a change in the pH of the reaction mixture was the cause for size variation of particles and the overall reaction rate, and they identified two different reaction pathways with the switching point at pH = 6.2−6.5.[7] For the reactions at low pH conditions (low citrate/tetrachloroauric acid ratio), which covers most of the traditional Frens's range for size variation,[6] the initial reaction rate is faster and the particles are formed through a nucleation−aggregation−smoothing pathway. In contrast, the reaction route at high pH conditions is slower and is consistent with the traditional nucleation−growth pathway.

While most reactions and the intermediates occurring during the formation of Au NPs are known, little work has been done to unravel the intricacies of the molecular mechanism of the initially crucial reduction of Au(III) and decarboxylation of citrate. A deep understanding of the molecular mechanism could lead to improvements and higher control over the experimental conditions. In this context, it is important to remark that many theoretical works have demonstrated the success of density functional theory (DFT) simulations to formulate models of molecular mechanisms on metal-mediated reactions[16] or on homogeneous catalysis.[17] Not only theoretical simulations have provided solid bases for the energetics of such processes and the geometries of reactants and products, but also have created the basis for new metal mediators and catalysts.[18] In the case of decarboxylation, the transformation consists of the extrusion of CO_2 mediated by a transition-metal, typically copper,[19,20] silver[21,22] or as described more recently, palladium.[23] All these decarboxylations have also been simulated by computational chemistry and their corresponding mechanisms have been uncovered.[24,25] Although gold-mediated mechanisms in decarboxylation processes have not been described yet, this metal recently has experienced much attention due to novel catalytic activities[26−28] and, for instance, in case of Au(III) the theoretical mechanism of the addition of water to propyne has been proposed.[29,30]

The aim of this combined theoretical and experimental article is 2-fold. First, we employed DFT calculations to investigate the energetics of the reduction of tetrachloroauric acid by sodium citrate at different pH mediums, as this is the rate-limiting step for Au NPs formation. Particularly, we are not only interested in the geometric structure of reactants, products, intermediates and transition states (TS) but also in the thermodynamics (reaction free energy) and kinetics (activation energy) of the reaction under different pH conditions. Second, we corroborated the theoretical findings with experimental assays of the Au NPs formation by monitoring the temporal evolution of the UV−vis absorption spectroscopy of the reaction solutions and TEM analysis of the final particle morphology. The ability to tune the reactivity and predict the size and dispersity of the final particles is of great importance for the manufacture of Au NPs in large-scale processes in a biocompatible and environmentally friendly manner. Therefore, quantification of energetic values and elucidation of the Au(III)-reduction mechanism would be of invaluable help to this aim.

II. METHODOLOGY

DFT Methodology. *Computational Procedure.* The geometry optimizations and TS calculations were carried out with the ADF2009 program using DFT.[31−33] The local density approximation (LDA), characterized by the electron-gas exchange, was used together with the Vosko−Wilk−Nusair (VWN) parametrization for correlation. Gradients were corrected by means of Becke and Perdew (BP) nonlocal corrections to the exchange and correlation energy, respectively. Triple-ζ and polarization (TZP) Slater basis sets were used to describe the valence electrons of all atoms. The inner core shells of C(1s), O(1s), Au (1s−4d), and Cl (1s−2p) were treated by the frozen core approximation. The ZORA formalism, implemented in DIRAC, with corrected core potentials was used to make relativistic corrections. This is especially important for heavy atoms such as Au. Default self-

consistent field (SCF) and geometry optimization convergence criteria were used.

Solvation effects were taken into account with conductor-like screening model (COSMO) approach[34] in which the solute molecule is embedded in a molecular-shaped cavity surrounded by a dielectric medium with given dielectric constant ε; in our case 78.4 for water solvent. Frequency calculations were also performed to identify all stationary points as minima (no imaginary frequency) or TS (only one imaginary frequency) and to also derive the thermal enthalpy and entropy corrections, allowing us to calculate finally reaction free energies (ΔG^R) and activation free energies ($\Delta G^\ddagger$) at the standard state of 298.15 K and 1 M.

Additional calculations have been carried out to assess the accuracy of the DFT/BP/TZP calculations. These calculations have been performed with Gaussian09 package[35] with the same procedure as the previous ones but with the use of the recent M06 functional developed by Truhlar.[36] This functional has become a good reference since it has demonstrated its good accuracy for the study of organometallic thermochemistry and kinetics. The standard 6-31G(d) basis set was used for light atoms while LANL2DZ effective core potential (ECP) was used for Au. Solvation energies were also included by means of the self-consistent reaction field (SCRF) method based on the polarizable continuum model (PCM) with radii and non-electrostatic terms derived by Truhlar and co-workers.[37]

Free Energy in Acid−Base Reactions. Special emphasis has to be taken into the calculation of the free energy of an acid−base reaction and their corresponding pK_a value. As exposed by Coote,[38] this simulation consists on a tough theoretical challenge due to the estimation of the hydration free energy of the H^+, whose value is under fierce debate.[39,40] To avoid this and others drawbacks Coote proposed to employ a thermodynamic cycle approach with a reference acid where the number of ionic species is conserved across the reaction and substantial cancellation errors incurred by the continuum solvent model can be expected. This approach has been assessed satisfactorily in the calculation of pK_a values of different classes of acids.[38] Here we have applied this approach with the use of the acetic acid (pK_a = 4.75) as reference acid. Likewise, we have avoided computing absolute pK_a values but relative ones to the experimental values of citric acid.

Experimental Details. *Reagents and Methods.* Sodium citrate and $HAuCl_4 \cdot 3H_2O$ were purchased from Sigma-Aldrich and stored under Ar atmosphere. Milli-Q water was used in all the experiments. UV−vis absorption spectra were recorded with a Cary 5 UV−vis−NIR spectrophotometer at room temperature. Au NPs were visualized using TEM (Tecnai F30) at an accelerating voltage of 200 kV. The sample (10 μL) was drop-cast onto ultrathin Formvar-coated 200-mesh copper grids (Tedpella, Inc.) and left to dry in air. For each sample, the size of at least 100 particles was measured to obtain the average and the size distribution. Each experiment was performed by triplicate and samples were stored in the fridge (+4 °C).

Synthesis of Au NPs. In a typical experiment, an aqueous solution of $HAuCl_4 \cdot 3H_2O$ (1 mL, 25 mM) was dissolved in H_2O (149 mL) in a three-neck round-bottom flask. The pH value of the solution was either left unmodified (to obtain a reaction mixture pH = 6.5) or the medium was acidified upon the addition of 0.1 M HCl (125 μL for pH = 5.6 or 250 μL for pH = 4.7). After heating up to 90 °C for 15 min, a solution of sodium citrate (0.1 g, 0.34 mM) in H_2O (1 mL) was added and the reaction mixture was maintained at the boiling temperature

for further time before an aliquot was taken and the reaction quenched by cooling the sample in ice−water.

III. RESULTS AND DISCUSSION

The pH Dependence of Reactive Species. Initially, it is crucial to review the structure dependence of the two reactants (tetrachloroauric acid and sodium citrate) on the pH of the medium in order to determine the dominant species at specific pH conditions. Actually, the dominant species are going to be the structures that mainly undertake the redox reaction. First, the strong tetrachloroauric acid totally dissociates in aqueous solutions generating a square planar $[AuCl_4]^-$ complex, which upon basic conditions progressively undergoes substitution of Cl^- ligands to form OH^--containing metallocomplexes, according to the reaction:

$$[AuCl_x(OH)_{4-x}]^- + OH^- \rightarrow [AuCl_{x-1}(OH)_{5-x}]^- + Cl^-$$
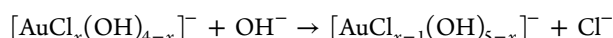
The dominance of each complex in solution was evaluated according to the pK constants of the successive equilibrium reactions ($pK_1 = 5.4$, $pK_2 = 6.4$, $pK_3 = 7.5$, and $pK_4 = 8.3$) extracted from Goia's work.[15] Similarly, the variation of the redox potential of sodium citrate in aqueous solution is associated with its ionization states,[41] whose pK_as values are 3.1 (for COOH next to OH), 4.8 and 6.4 (for both COOH far from OH),[7] and 14.4 (for OH).[42] From both series of pK constants it is not difficult to deduce the dominant species of both reactants depending on the pH (Table 1). Amid all ranges,
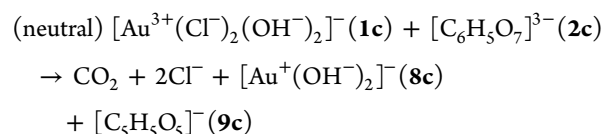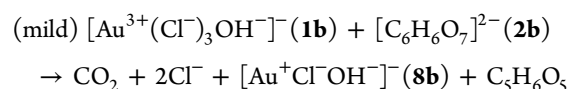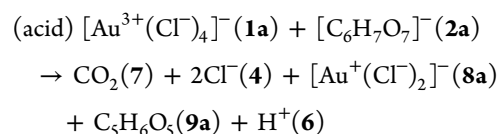
Table 1. Dominant Structure of the Aureate Complex and Citrate Ions Depending on the pH of the Medium

pH ranges originated from pK	dominant structure of citrate	dominant structure of the aureate	studied medium
<3.1	$C_6H_8O_7$	$[AuCl_4]^-$	–
3.1−4.8	$[C_6H_7O_7]^-$	$[AuCl_4]^-$	acid
4.8−5.4	$[C_6H_6O_7]^{2-}$	$[AuCl_4]^-$	–
5.4−6.4	$[C_6H_6O_7]^{2-}$	$[AuCl_3OH]^-$	mild acid
6.4−7.5	$[C_6H_5O_7]^{3-}$	$[AuCl_2(OH)_2]^-$	neutral
7.5−8.3	$[C_6H_5O_7]^{3-}$	$[AuCl(OH)_3]^-$	–
>8.3	$[C_6H_5O_7]^{3-}$	$[Au(OH)_4]^-$	–

we centered our interest in the acidic (3.1−4.8) and mild acidic conditions (5.4−6.4), as these are approximately the conditions studied by Frens,[6] as well as in the neutral medium (6.4−7.5) studied by Peng and co-workers.[7] In more detail, under acidic conditions only the single deprotonated citrate species exists together with the fully chlorinated Au(III)-complex, while under mild acidic conditions only one carboxylic acid remains in the citrate and one hydroxyl group has entered into the Au(III) complex. Finally under neutral medium we obtained the combination of the fully deprotonated citrate with the dihydroxylated Au(III) complex.

The Proposed Mechanism of the Au(III) Reduction by Citrate. We have previously postulated a possible reaction mechanism for the reduction of Au(III) species by sodium citrate based on (a) experiments about the effect of the isotopic replacement of the solvent[10] and (b) an existing experimental mechanism proved for the reduction of Au(III) by the oxalate anion.[43,44] On the roots of these experiments and also the findings of the present theoretical research, we propose a general mechanism for the overall redox reaction according to the pH conditions with the following stoichiometries where

numbers denotes the type of compound and letters the variant in each medium (a, acid; b, mild acid; c, neutral):

$$\text{(acid) } [Au^{3+}(Cl^-)_4]^- \, (\mathbf{1a}) + [C_6H_7O_7]^- \, (\mathbf{2a})$$
$$\rightarrow CO_2 \, (\mathbf{7}) + 2Cl^- \, (\mathbf{4}) + [Au^+(Cl^-)_2]^- \, (\mathbf{8a})$$
$$+ C_5H_6O_5 \, (\mathbf{9a}) + H^+ \, (\mathbf{6})$$

$$\text{(mild) } [Au^{3+}(Cl^-)_3OH^-]^- \, (\mathbf{1b}) + [C_6H_6O_7]^{2-} \, (\mathbf{2b})$$
$$\rightarrow CO_2 + 2Cl^- + [Au^+Cl^-OH^-]^- \, (\mathbf{8b}) + C_5H_6O_5$$

$$\text{(neutral) } [Au^{3+}(Cl^-)_2(OH^-)_2]^- \, (\mathbf{1c}) + [C_6H_5O_7]^{3-} \, (\mathbf{2c})$$
$$\rightarrow CO_2 + 2Cl^- + [Au^+(OH^-)_2]^- \, (\mathbf{8c})$$
$$+ [C_5H_5O_5]^- \, (\mathbf{9c})$$

The most favorable reaction path involves a decarboxylation in four main steps (Figure 1). First, an initial Cl^--substitution in the Au(III) complex by a citrate molecule, which, whatever the pH, has to react through the carboxylate group attached to the hydroxyl carbon in order to proceed with the reaction. Second, and only in the acidic medium, a deprotonation of the second most acidic group in citrate via an acid−base reaction since the coordination of the metal unit changes slightly the acid−base properties of this carboxylic group. This step is unnecessary in mild and neutral pH mediums as this group is already deprotonated. The third step simply consists in an internal conversion of the Au equatorial coordination from the initial carboxylate ligand to the hydroxyl group. This step paves the way for the formation of the transition state. Finally, the fourth step involves the formation of the TS and the concerted decarboxylation and electron transfer from citrate to Au(III), which is the rate-limiting step due to the elevated cost for C−C breaking.

The free energy for all four reactions and the formation of the TS in the three considered pH mediums are reported in Table 2. The overall energy profile of the proposed path at acidic and neutral pH is displayed graphically in Figure 2 and the main structures are shown in Figure 3. The total reaction free energy is highly exergonic (from −26.5 to −37.2 kcal/mol) in all three conditions due to the favorable contribution (from −46.4 to −58.4 kcal/mol) of the decarboxylation, whereas the other three steps are fully endergonic, specially the ligand substitution step (from +17.4 to +19.9 kcal/mol). However, the kinetics of the reaction are controlled by the activation free energy that is computed to be +26.8 kcal/mol in acidic medium and significantly higher in mild acidic and neutral mediums, +34.0 and +37.4 kcal/mol, respectively. These values are similar in magnitude to the activation energy of the benzannulation-catalyzed reaction by Au(III)[30] and also to the activation energies of decarboxylation by other metals like Cu,[19] Ag,[21] and Pd.[23] These differences explain the distinct reactivity profile of the reaction depending on the pH. It is important to remark that the reaction free energy of the formation of the TS is responsible of the observed different energy profile. In acidic medium this energy accounts for 59−68% lower cost than in either mild acidic or neutral conditions. The causes of such differentiation are pinpointed by an accurate analysis of the activation energy for each step and especially for the formation of the TS (*vide infra*).

Substitution of a Cl^- Ligand by a Citrate Molecule (Step 1). Although the initial ligand substitution reaction in the

23684

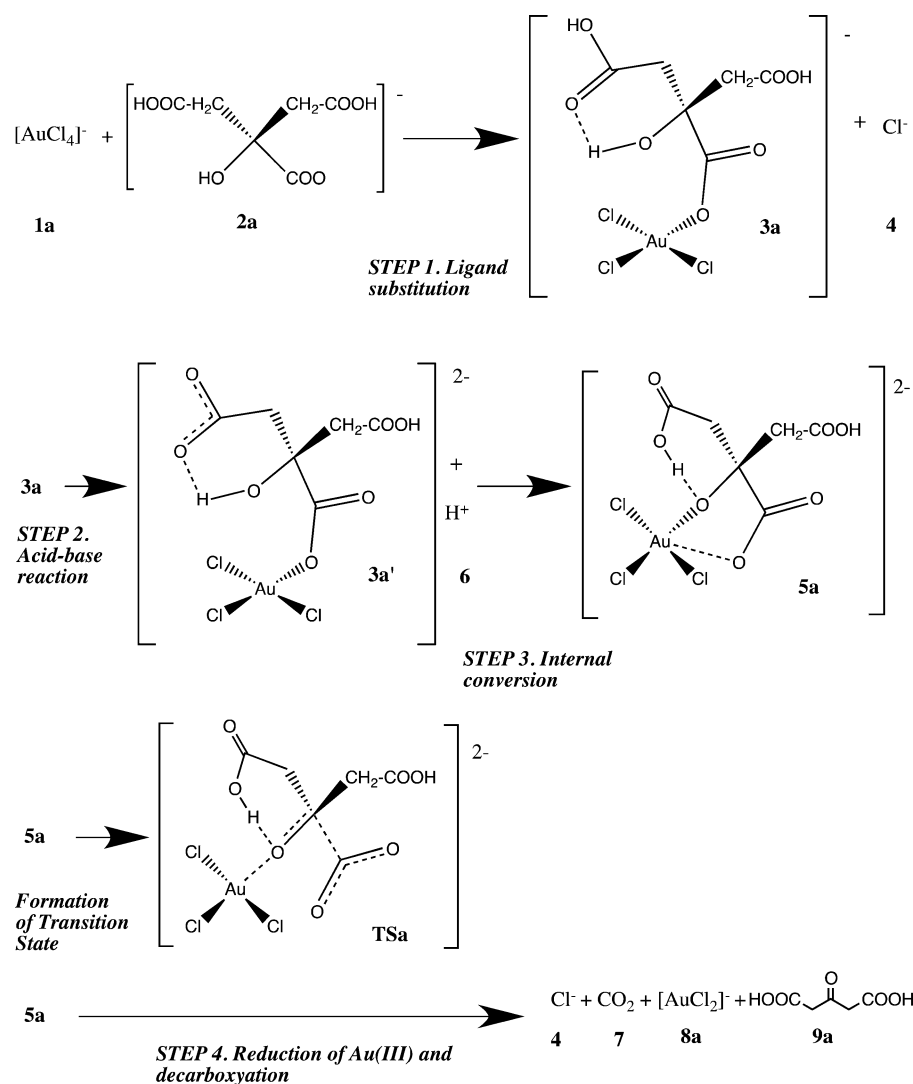dx.doi.org/10.1021/jp305830p | J. Phys. Chem. C 2012, 116, 23682−23691

Figure 1. Proposed mechanism of the reduction of Au(III) by the oxidation of the citrate at acid medium (pH 3.1–4.8) comprised by 10 compounds and one TS. See Figure 2 for the free energy profile and Figure 3 for the geometric structures. The mechanism in mild acid and neutral conditions is just slightly different, see Supporting Information section.
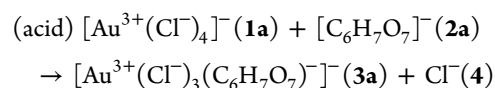
Table 2. Decomposition of the Total Free Energy (ΔG^R) and Activation Free Energy ($\Delta G^{\ddagger}$) of the Reduction of Au(III) by Citrate in Several pH Medium (kcal/mol)[a]

	acid	mild acid	neutral
step 1. ligand substitution	18.6	17.4	19.9
step 2. acid−base	−0.1	-	-
step 3. internal conversion	2.7	3.0	0.0
formation of the transition state	5.6 (6.3)	13.6 (13.0)	17.5 (17.8)
step 4. decarboxylation and reduction of Au(III)	−58.4	−49.9	−46.4
activation free energy, $\Delta G^{\ddagger}$ (step 1 + step 2 + step3 + TS Formation)	26.8	34.0	37.4
total reaction free energy, ΔG^R (step 1 + step 2 + step 3 + step 4)	−37.2	−29.5	−26.5

[a] Energies are computed with DFT/BP except those in parentheses that correspond to DFT/M06.

Au(III) complex is irrelevant in terms of final energetic differentiation, this step is crucial in order to form a complex where the reducing agent (citrate) and the oxidizing agent (auric complex) coexist. As the dominant species for the citrate and the Au(III) complex are strongly dependent on the pH of

the medium, the expected substitutions reactions are slightly different according to the following options:
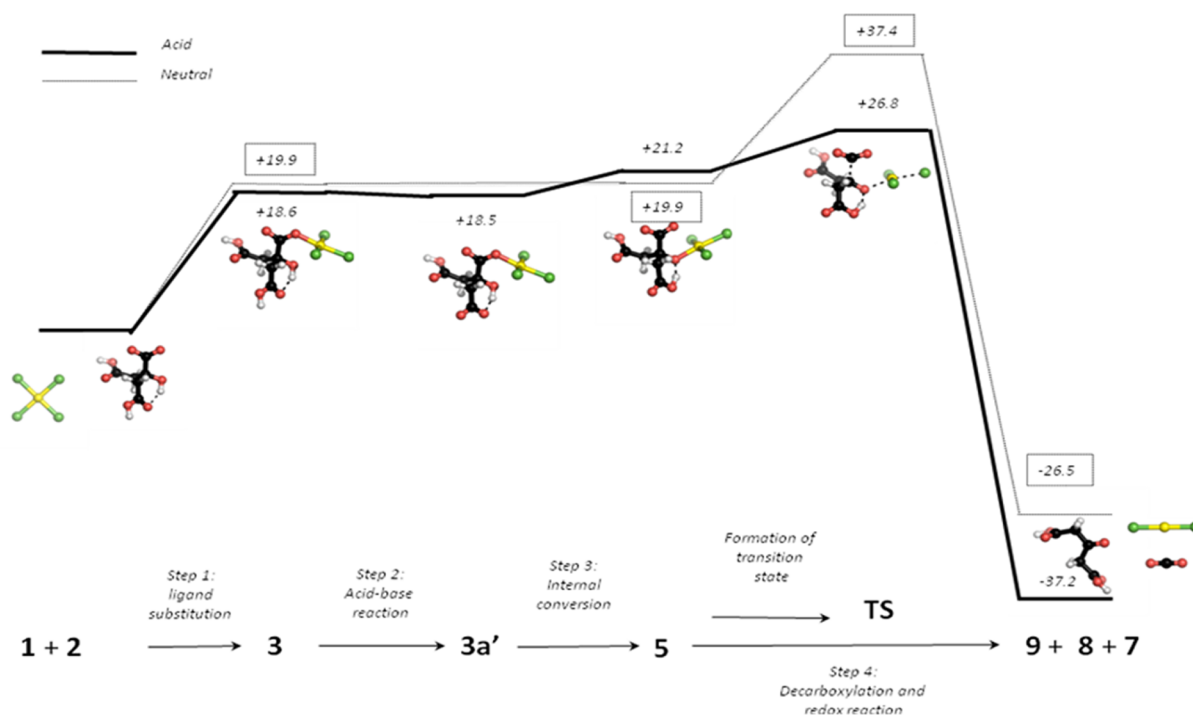
$$(\text{acid}) \; [Au^{3+}(Cl^-)_4]^- (\mathbf{1a}) + [C_6H_7O_7]^- (\mathbf{2a})$$
$$\rightarrow [Au^{3+}(Cl^-)_3(C_6H_7O_7)^-]^- (\mathbf{3a}) + Cl^- (\mathbf{4})$$

Figure 2. Energy profile at DFT/BP/TZP of the proposed reaction pathway of the reduction of Au(III) by citrate at acid and neutral mediums in kcal/mol. The main intermediates and the highest transition state structure are also displayed for acid conditions only. The dashed lines in the structure represent either an intramolecular hydrogen bond or the disintegrating bonds in the TS. The structure **3a′** is only involved in acidic medium.
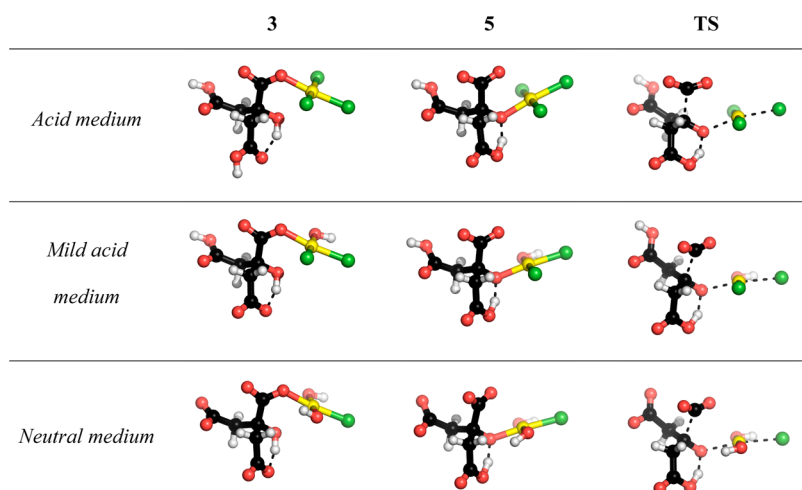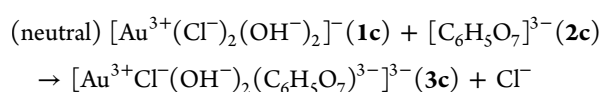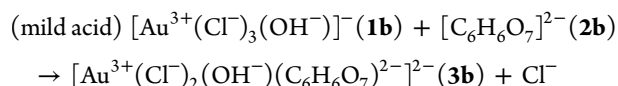

Figure 3. Ball and stick models, rendered with Pymol,[45] of the most relevant structures involved in the decarboxylation of citrate mediated by Au(III) in the three pH conditions studied. The dashed lines represent either an intramolecular hydrogen bond or the disintegrating bonds in the TS.

(mild acid) $[Au^{3+}(Cl^-)_3(OH^-)]^-$ (**1b**) + $[C_6H_6O_7]^{2-}$ (**2b**)

$\rightarrow [Au^{3+}(Cl^-)_2(OH^-)(C_6H_6O_7)^{2-}]^{2-}$ (**3b**) + Cl^-

(neutral) $[Au^{3+}(Cl^-)_2(OH^-)_2]^-$ (**1c**) + $[C_6H_5O_7]^{3-}$ (**2c**)

$\rightarrow [Au^{3+}Cl^-(OH^-)_2(C_6H_5O_7)^{3-}]^{3-}$ (**3c**) + Cl^-

The reaction is unfavorable in all three pH conditions though differences are small (<2.5 kcal/mol). From the free energies of ligand substitutions for all possible combinations of reactants in Table 3, one can deduce that the increasing cost of Cl^- substitution from acidic to neutral medium can be attributed mainly to the increasing number of OH^- ligands in the auric species that strengthen the remaining Au−Cl bonds. This is in agreement with previous studies by Raman and UV−vis spectroscopy of successive replacement of chloride by hydroxide ligands in Au(III) species.[46] Besides, it could be observed an opposite effect when considering the citrate ligand, since the species under acidic conditions, $[C_6H_7O_7]^-$, require more energy than in neutral medium, $[C_6H_5O_7]^{3-}$, to undergo ligand substitution in Au(III) species. However, it is reasonable to assume that substitution is favored by highly charged protonation states of citrate.

Table 3. Hypothetical Reaction Free Energy of the Ligand Substitution (ΔG^R, Step 1) Reaction Between All Possible Reactants (kcal/mol)[a]
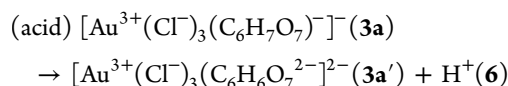
	$[C_6H_7O_7]^-$	$[C_6H_6O_7]^{2-}$	$[C_6H_5O_7]^{3-}$
$[AuCl_4]^-$	18.6	16.6	15.3
$[AuCl_3OH]^-$	20.4	17.4	16.8
$[AuCl_2(OH)_2]^-$	22.6	20.6	19.9

[a]We use the hypothetical adjective since some of the combinations cannot coexist simultaneously at the same pH conditions, but their calculation help us to elucidate the mechanism. The only considered isomers are those that the carboxylate near to the hydroxyl coordinates the Au metal and contains a Cl ligand *trans* to it.

While under acidic conditions only one substitution reaction over **3** is possible, in both mild acidic and neutral mediums several isomers are possible but finally restrained by the fact that Cl⁻ substituent is always the most labile and the one readily to leave, either in $[AuCl_3OH]^-$ (mild acidic) and in $[AuCl_2OH_2]^-$ (neutral) species. For instance, the substitution of Cl⁻ by OH⁻ in $[AuCl_3OH]^-$ is favored by −24.8 kcal/mol and the subsequent substitution by −23.1 kcal/mol. It should be noted that OH⁻ is a bad leaving group compared to Cl⁻ for Au(III) complexes.[47] In all the cases, the coordination of citrate proceeds via the unprotonated oxygen of the most acidic carboxylic acid (the one next to the OH⁻ in **2**) since only this conformation can form a favorable 5-membered ring TS with the participation of the nearby hydroxyl. Also constrained by the TS requirements is the selection of the isomer where the citrate is located in *trans* position to a Cl⁻ ligand in order to facilitate the future decarboxylation (see Figure 3 in the molecular models).

To sum up, the main geometrical features of the resulting metallocomplex **3** after ligand substitution reaction regardless the pH are (Figure 3): (i) the metallocomplex always keeps its initial square planar structure typical for Au(III) complexes,[48] (ii) Au(III) atom coordinates with the carboxylate group of citrate close to the hydroxyl, (iii) citrate is located in *trans* position to a Cl⁻ ligand, (iv) an intramolecular hydrogen bond between the hydroxyl group and one carboxylic/carboxylate groups is formed to give a 6-membered ring, and (v) the orientation of the OH⁻ ligands is insignificant to the final energetics.

An Acid−Base Reaction to Deprotonate the Second Most Acidic Carboxylic Group (in Acidic Medium Only, Step 2). Assuming that coordination to a metallic atom such as Au(III) could slightly modify the pK_as of citrate, we first studied their acid−base properties. Only the second most acidic carboxylic group is expected to be deprotonated in acidic medium, while the same intermediate structures **3** in the mild acidic and neutral mediums remain unaltered. The stoichiometry of the acid−base reaction in acidic medium is as follows:

$$\text{(acid) } [Au^{3+}(Cl^-)_3(C_6H_7O_7)^-]^- \ (\mathbf{3a})$$
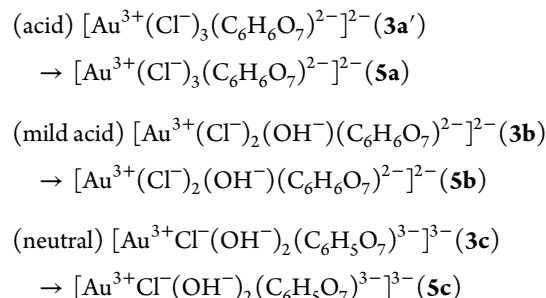$$\rightarrow [Au^{3+}(Cl^-)_3(C_6H_6O_7{}^{2-})^{2-}]^{2-}(\mathbf{3a'}) + H^+ (\mathbf{6})$$

The present calculations indicate that the coordination of the metallic unit to citrate increases the acidity of the carboxylic groups, though the effect is not constant for all mediums.[43] In acidic medium, once citrate is coordinated by the metallic unit, the energy cost of the deprotonation of the second most acidic group (the COOH near OH) is computed to be marginally favorable by −0.1 kcal/mol, which represents a relative decrease

of the experimental pK_a value from 4.8 to 3.1. On the other hand, although a reduction of the pK_a values for the rest of acidic groups (decrease of 0.9 units for the remaining COOH and of 2.9 units for the hydroxyl group) is predicted, deprotonation does not actually proceed due to the acidic pH conditions. Therefore, at this pH range (3.1−4.8), it is predicted that the most favorable reaction pathway proceeds via deprotonation of the second most acidic carboxylic group.

On the other hand, no deprotonation reactions are predicted to occur under mild acidic or neutral mediums since the reduction of the pK_a values is not significant to ensure a change of the protonated species. For instance, in mild acidic medium the predicted decrease of the pK_a value of the remaining carboxylic group is computed to be of 0.4 pK_a units only, whereas in neutral medium there is no acidification effect since carboxylic acids are already deprotonated. In these both cases we assume that the initially coordinated structures **3** proceed with the decarboxylation reaction without any additional acid−base reaction.

An Internal Conversion To Prepare the Geometry for the Transition State (Step 3). The initial coordination of the Au(III) metallic center to the carboxylate of citrate (compound **3**) requires a change of coordination to the nearby hydroxyl group (compound **5**) in order to facilitate the formation of the transition state. The energy reaction corresponding to the internal transformation of **3a′**/**3** to **5** is as follows:

$$\text{(acid) } [Au^{3+}(Cl^-)_3(C_6H_6O_7)^{2-}]^{2-}(\mathbf{3a'})$$
$$\rightarrow [Au^{3+}(Cl^-)_3(C_6H_6O_7)^{2-}]^{2-}(\mathbf{5a})$$

$$\text{(mild acid) } [Au^{3+}(Cl^-)_2(OH^-)(C_6H_6O_7)^{2-}]^{2-}(\mathbf{3b})$$
$$\rightarrow [Au^{3+}(Cl^-)_2(OH^-)(C_6H_6O_7)^{2-}]^{2-}(\mathbf{5b})$$

$$\text{(neutral) } [Au^{3+}Cl^-(OH^-)_2(C_6H_5O_7)^{3-}]^{3-}(\mathbf{3c})$$
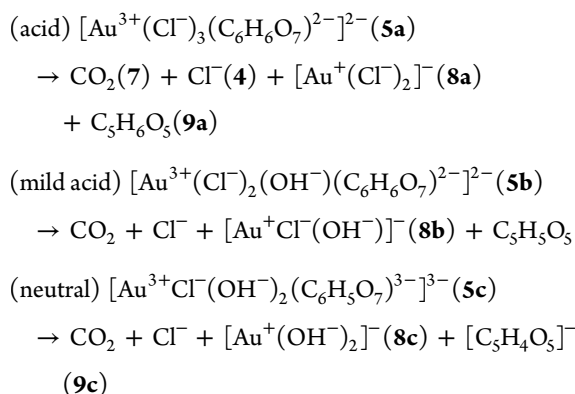$$\rightarrow [Au^{3+}Cl^-(OH^-)_2(C_6H_5O_7)^{3-}]^{3-}(\mathbf{5c})$$

This endergonic step has little consequences in the differences of activation energies due to the low cost of this transformation, from 0.0 to 3.0 kcal/mol only.

From the geometrical point of view, it is worth to mention that the structure of the pentacoordinated metallocomplex **5** (see Figure 3) maintains the square-planar conformation while favors the equatorial coordination of the new keto oxygen, rather than the initial carboxylate moiety, which now adopts a slightly axial position as suggested elsewhere.[49,50] Thus, the carboxylate−Au distance, on average, evolves from 2.07 Å in **3a′**/**3b**/**3c** to 2.76 Å in **5**, whereas the opposite trend is found for the hydroxyl−Au distance, from 2.77 to 2.08 Å. This fact leads to a more flexible carboxylate group readily to leave as a CO_2 molecule at the end of the reaction. Simultaneously, after the new coordination of the hydroxyl group to the Au(III) metal the hydrogen is finally transferred to the carboxylate, with which was forming an intramolecular hydrogen bond. This fact is revealed by the shortening of the distance between the carboxylate and the hydrogen (1.05 Å) and the lengthening of the distance between such hydrogen and the former hydroxyl oxygen (1.47 Å). In this way, the initial hydroxyl oxygen becomes more a keto oxygen resembling to the final product of the reaction. This kind of proton transfer through a hydrogen bond has been reported also in other systems.[51,52]

The Energy Cost of TS Formation as a Function of Au−Cl Strength (Step 4). In the final stage, decarboxylation

of the coordinated metallocomplex **5** leads to the following products depending on the pH of the medium:

(acid) $[Au^{3+}(Cl^-)_3(C_6H_6O_7)^{2-}]^{2-}$ (**5a**)

$\rightarrow CO_2$ (**7**) $+ Cl^-$ (**4**) $+ [Au^+(Cl^-)_2]^-$ (**8a**)

$+ C_5H_6O_5$ (**9a**)

(mild acid) $[Au^{3+}(Cl^-)_2(OH^-)(C_6H_6O_7)^{2-}]^{2-}$ (**5b**)

$\rightarrow CO_2 + Cl^- + [Au^+Cl^-(OH^-)]^-$ (**8b**) $+ C_5H_5O_5$

(neutral) $[Au^{3+}Cl^-(OH^-)_2(C_6H_5O_7)^{3-}]^{3-}$ (**5c**)

$\rightarrow CO_2 + Cl^- + [Au^+(OH^-)_2]^-$ (**8c**) $+ [C_5H_4O_5]^-$

(**9c**)

As expected, this reaction is highly exergonic due to the breaking of the C–C bond to release CO_2. It also contains the highest TS of the overall reaction, which in turn determines the rate-limiting step. The activation energy is significantly lower in acidic conditions by approximately a minimum of 7 kcal/mol compared to the other pH conditions and therefore it is responsible for the different reactivity of the overall redox reaction. Apart from the DFT/BP/TZP energies, we have also assessed the accuracy of the crucial formation of the transition state by the recent DFT/M06 functional (See values in parentheses in Table 2). The absolute mean error between the three magnitudes is only 0.9 kcal/mol and the energetic differences among the three mediums are kept almost intact and therefore the DFT/M06 validates the present DFT/BP/TZP energetic profile.

The increasing energy cost of TS formation from acid to neutral (+5.6 to +19.4 kcal/mol, respectively) can be associated with the extrusion of the *trans* Cl^-, whose bond with Au is largely weakened in the TS. Actually, the energy cost of the TS formation is correlated with a change of the metallocomplex structure rather than with a change of the protonation state of citrate according to Table 4. In line with this, although the *trans*

Table 4. Hypothetical Free Energy of the Formation of the Transition State ($\Delta G^{\ddagger}$) in All Possible Complexes (kcal/mol)[a]

	$[C_6H_6O_7]^{2-}$	$[C_6H_5O_7]^{3-}$
$[AuCl_4]^-$	5.6	5.8
$[AuCl_3OH]^-$	13.6	12.7
$[AuCl_2(OH)_2]^-$	18.0	17.5

[a]Isomers derived from those in Table 3. Data for $[C_6H_6O_7]^-$ is not presented since the mechanism converge to that of $[C_6H_6O_7]^{2-}$ after the initial acid–base reaction.

Au–Cl bond length in **5** is almost invariant for all three mediums (2.36, 2.35, and 2.35 Å for acid, mild acid, and neutral, respectively), the same distance in the TS structure increases consecutively with the cost of TS formation to 2.53, 2.59, and 2.63 Å, respectively. This is indicative that neutral and mild acidic medium requires higher distortion to the complex **5** to achieve the TS than the acidic one.

From the geometrical point of view, the disintegration of the intermediate **5** into products requires the formation of a cyclic 5-membered ring TS, where the citrate substituent is located *trans* to a Cl^- ligand. No other conformers were able to reach a proper TS. So, as the Cl^- substituent is much more labile than

OH^-, decarboxylation at high basic medium, where $[AuOH_4]^-$ is the predominant form, is predicted to be highly unfavorable. This is also supported by a recent report, which found that at least one Cl^- ligand is necessary at the Au(III) center to catalyze the addition of water to propyne.[53] The TS also reinforces the role of the *trans* Cl^- atom as a leaving group while Au(III) cation is reduced to Au(I), which tends to form linear rather than square planar complexes.[54] The typical features of these TS structures are as follows: (i) lengthening of the *trans* Au–Cl bond (+0.23 Å on average for all three pH mediums compared to **5**) and the Au–O bond (+0.24 Å), (ii) lengthening of the C–CO_2 bond from 1.56 Å in **5** to a common 2.08 Å in the TS (on average), as seen in other decarboxylation mechanism,[25] (iii) maintenance of the *cis* Au–Cl and Au–OH bond lengths, (iv) shortening of the C–O bond toward a typical distance of a carbonyl group in a ketone (1.32 Å on average), and, (v) finally, the planarization of the keto carbon to a more sp^2–like hybridization. Additionally, TS also includes the formal 2-electron transfer from the keto oxygen to the Au(III) atom, which is deduced by the decrease of the Mulliken electron charge from +0.98 in **5** to +0.69 in the TS (as average in all mediums), an effective 0.29 electron transfer, and by the formation of a common linear Au(I) complex. The computation of the free energy of the TS formation completes the calculation of overall activation free energy, which determines the kinetics of the overall reduction of tetrachloroauric acid.

Synthesis of Au NPs Favored in Acid Medium. Experimental evidence supporting theoretical calculations were obtained from the kinetics of formation of Au colloids based on the time evolution of the Surface Plasmon Resonance (SPR) band in the UV–vis spectra. The syntheses of Au NPs formation were performed under the same reaction conditions (sodium citrate/$HAuCl_4$ = 13.6, $[HAuCl_4]$ = 0.165 mM) but systematically decreasing the pH of the initial reaction mediums upon addition of 0.1 M HCl. Since the Au NPs evolution rate is dependent on the temperature, reactions were run at 90 °C, thus proceeding at slow rates and facilitating the study of the initial stages of the reaction. Temporal evolution of the particle formation has been recorded as a function of time after the initiation event, which is the addition of citrate to the precursor solution containing $HAuCl_4$ (direct addition).[8] The reaction was quenched by cooling the samples in ice–water. In order to verify that quenching does indeed provide sufficient delay for sampling, two samples were collected during the reaction in which one sample was quenched and later (about 1 h) analyzed and the other sample was analyzed immediately. In both cases the spectra compared well. Extended UV–vis spectra comparing the Au NP evolutions obtained following the three different conditions (acidic, mild acidic and neutral) are plotted in Figure 4.

Comparing Au NP kinetics, it can be clearly seen how the time scale strongly depends on the pH of the solution. In detail, kinetics of Au NP formation is faster in the case of acidic medium of pH = 4.7 (~3 min to complete reaction) than under mild acidic conditions at pH = 5.6 (~5 min to reach completion), while when the pH of the initial reaction solution was neutral (pH = 6.5) the reaction could not be completed after more than 7 min. TEM and image analysis of the final Au NPs after 7 min clearly confirmed a decrease of the mean particle size as a consequence of decreasing the pH of the medium (Figure 5). Therefore, acidic and mild acidic conditions lead to the production of smaller sized Au NPs
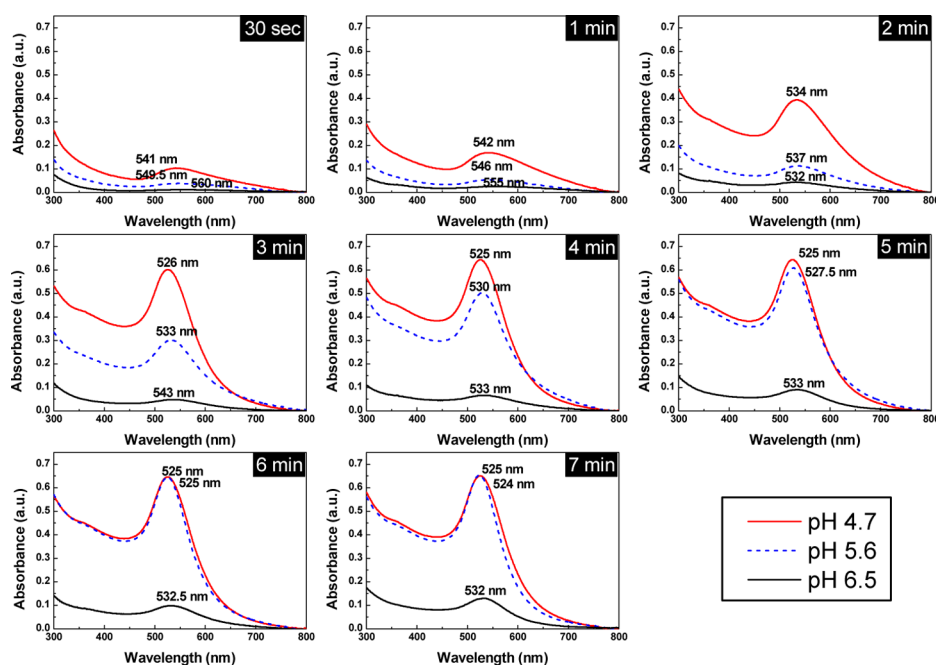
Figure 4. Time evolution of the UV−vis absorbance spectra of Au NPs synthesized at conditions of 0.165 mM of $HAuCl_4$ and a sodium citrate:$HAuCl_4$ ratio of 13.6 at 90 °C, under acidic, mild acidic and neutral conditions. The appearance of a peak at ∼525 nm is characteristic of the SPR of Au colloids.
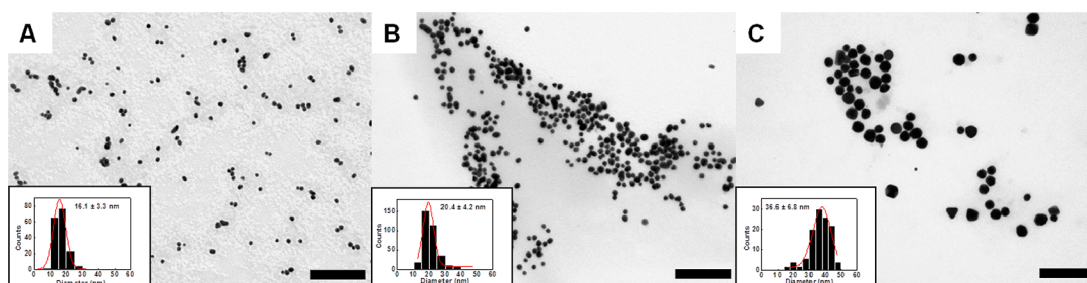

Figure 5. Morphological (TEM) characterization of Au NPs synthesized at conditions of 0.165 mM of $HAuCl_4$ and a sodium citrate:$HAuCl_4$ ratio of 13.6 at 90 °C after 10 min under acidic (A), mild acidic (B), and neutral pH conditions (C). Scale bars are 200 nm.

with narrower size distributions (16.1 ± 3.3 and 20.4 ± 4.1 nm in diameter, respectively), in comparison with those obtained in the case of neutral pH (36.6 ± 6.8 nm). These results are in agreement with previous studies, which reported that smaller sizes of Au NPs are generally a consequence of a faster reduction.[10] A faster reduction quickly leads to a supersaturated solution and a high nucleation rate, which depletes the solution of available precursor atoms for growth, leading to smaller particles.

IV. FINAL REMARKS AND CONCLUSIONS

The mechanism of the reduction of Au(III) by citrate to form Au NPs has been analyzed in detail. Previous assumptions and experimental evidence have now been corroborated with theoretical calculation of energetic costs of the proposed mechanism. An exhaustive comparison between the mechanisms in three different pH conditions has been disclosed. The differences in these mechanisms support the finding that the more acidic the medium the faster the reduction rate. So, the theoretical trends agree with experimental observations of the kinetics of Au NP formation, characterized by UV−vis spectroscopy and TEM.

The base of the different reactivities has its roots in the distinct protonation state of the citric acid and the different number of OH^- ligands inserted into the Au(III) complex depending on the pH of the medium. The activation energy, which determines the kinetics of the reaction, can be dissected into four distinct steps in the most favorable reaction path: (i) substitution of a Cl^- by a citrate ligand in the auric acid, (ii) deprotonation of the second most acid carboxylic group (only in acidic medium conditions), (iii) internal conversion from equatorial coordination of Au(III) to carboxylate to the hydroxyl oxygen, and (iv) formation of a 5-membered ring TS that lead to the final products (i.e., CO_2, dicarboxyacetone, Cl^-, and Au(I) complex). On the one hand, ligand substitution and TS formation, which compute the 90% of the total activation energy, are mainly favored by Au(III) complexes with low number of Cl^- ligands (case where Cl^- is much more labile), whereas the change in the citrate protonation state has a much lower effect on the energetics of the activation energy. On the other hand, the two remaining steps, although necessary, have a much lower impact in the activation energy. Without taking into account the effect of the number of Cl^- ligands in the Au(III) complex, the deprotonation of the citrate moderately favors the decrease of the activation energy, as seen

in ligand substitution especially. This fact suggests the key idea that a citrate molecule with lower pK_a values (i.e., more acidic) will promote a faster reduction under similar pH conditions.

Ongoing work focuses on translating the higher reactivity observed in acidic pH medium into mild acidic and neutral conditions by employing derivatives of sodium citrate, which could increase the reduction rate of tetrachloroauric acid while maintaining their role as NP stabilizers and ensuring their compatibility with the reduction system. Therefore, a range of suitable candidates are those having electron-withdrawing substituents that could reduce the pK_a value of the carboxylic groups therefore allowing the generation of deprotonated citrate molecules at lower pH values.

■ ASSOCIATED CONTENT

Ⓢ Supporting Information

Detailed mechanisms in mild acid and neutral conditions, DFT/BP/TZP optimized geometries, enthalpies, entropies, and free energies for all main compounds in the three medium conditions. This material is available free of charge via the Internet at http://pubs.acs.org.

■ AUTHOR INFORMATION

Corresponding Author
*E-mail: campanera@ub.edu, Telephone +34934035985, Fax: +34934035987.

Notes
The authors declare no competing financial interest.

■ ACKNOWLEDGMENTS

■ REFERENCES

(1) *Standard Reference Materials*. http://www.nist.gov/srm (accessed May 15, 2012).
(2) Daniel, M.; Astruc, D. *Chem. Rev.* **2004**, *104*, 293−346.
(3) Dreaden, E. C.; Alkilany, A. M.; Huang, X.; Murphy, C. J.; El-Sayed, M. A. *Chem. Soc. Rev.* **2012**, *41*, 2740−2779.
(4) Turkevich, J.; Stevenson, P. C.; Hillier, J. *Discuss. Faraday Soc.* **1951**, *11*, 55−75.
(5) Turkevich, J.; Stevenson, P. C.; Hillier, J. *J. Phys. Chem.* **1953**, *57*, 670−673.
(6) Frens, G. *Nature Phys. Sci.* **1973**, *241*, 20−22.
(7) Ji, X.; Song, X.; Li, J.; Bai, Y.; Yang, W.; Peng, X. *J. Am. Chem. Soc.* **2007**, *129*, 13939−13948.
(8) Ojea-Jimenez, I.; Bastus, N. G.; Puntes, V. *J. Phys. Chem. C* **2011**, *115*, 15752−15757.
(9) Sivaraman, S. K.; Kumar, S.; Santhanam, V. *J. Colloid Interface Sci.* **2011**, *361*, 543−547.
(10) Ojea-Jimenez, I.; Romero, F. M.; Bastus, N. G.; Puntes, V. *J. Phys. Chem. C* **2010**, *114*, 1800−1804.
(11) Lamer, V. K.; Dinegar, R. H. *J. Am. Chem. Soc.* **1950**, *72*, 4847−4854.
(12) Chow, M. K.; Zukoski, C. F. *J. Colloid Interface Sci.* **1994**, *165*, 97−109.
(13) Rodriguez-Gonzalez, B.; Mulvaney, P.; Liz-Marzan, L. M. *Z. Phys. Chem.* **2007**, *221*, 415−426.
(14) Gammons, C. H.; Yu, Y. M.; WiliamsJones, A. E. *Geochim. Cosmochim. Acta* **1997**, *61*, 1971−1983.
(15) Goia, D. V.; Matijevic, E. *Colloids Surf., A* **1999**, *146*, 139−152.
(16) Torrent, M.; Solà, M.; Frenking, G. *Chem. Rev.* **2000**, *100*, 439−493.

(17) van Leeuwen, P. W. N. M. ; Morokuma, K. ; van Lenthe, J. H. *Theoretical Aspects of Homogeneous Catalysis: Applications of ab initio Molecular Orbital Theory*; Kluwer Academic Publishers: Dordrecht, The Netherlands, Boston, MA, and London, 1995; p 217.
(18) Zipoli, F.; Car, R.; Cohen, M. H.; Selloni, A. *J. Chem. Theory Comput.* **2010**, *6*, 3490−3502.
(19) Goossen, L. J.; Manjolinho, F.; Khan, B. A.; Rodríguez, N. *J. Org. Chem.* **2009**, *74*, 2620−2623.
(20) Bi, H.; Zhao, L.; Liang, Y.; Li, C. *Angew. Chem., Int. Ed.* **2009**, *48*, 792−795.
(21) Gooßen, L.; Rodríguez, N.; Linder, C.; Lange, P.; Fromm, A. *ChemCatChem* **2010**, *2*, 430−442.
(22) Grainger, R.; Nikmal, A.; Cornella, J.; Larrosa, I. *Org. Biomol. Chem.* **2012**, *10*, 3172−3174.
(23) Zhang, F.; Greaney, M. F. *Angew. Chem., Int. Ed.* **2010**, *49*, 2768−2771.
(24) Dupuy, S.; Lazreg, F.; Slawin, A. M. Z.; Cazin, C. S. J.; Nolan, S. P. *Chem. Commun.* **2011**, *47*, 5455−5457.
(25) Zhang, S. -.; Fu, Y.; Shang, R.; Guo, Q.; Liu, L. *J. Am. Chem. Soc.* **2010**, *132*, 638−646.
(26) Hashmi, A. S. K.; Rudolph, M. Gold catalysis in total synthesis. *Chem. Soc. Rev.* **2008**, *37*, 1766−1775.
(27) Rudolph, M.; Hashmi, A. S. K. *Chem. Soc. Rev.* **2012**, *41*, 2448−2462.
(28) Nolan, S. P. *Nature* **2007**, *445*, 496−497.
(29) Lein, M.; Rudolph, M.; Hashmi, S. K.; Schwerdtfeger, P. *Organometallics* **2010**, *29*, 2206−2210.
(30) Straub, B. F. *Chem. Commun.* **2004**, *10*, 1726−1728.
(31) te Velde, G.; Bickelhaupt, F. M.; Baerends, E. J.; Fonseca Guerra, C.; van Gisbergen, S. J. A.; Snijders, J. G.; Ziegler, T. *J. Comput. Chem.* **2001**, *22*, 931−967.
(32) Fonseca-Guerra, C.; Snijders, J. G.; Te Velde, G.; Baerends, E. J. *Theor. Chem. Acc.* **1998**, *99*, 391−403.
(33) SCM, *Theoretical Chemistry*; Vrije Universiteit: Amsterdam, The Netherlands, http://www.scm.com ADF2009.01.
(34) Pye, C. C.; Ziegler, T.; Lenthe, E. V.; Louwen, J. N. *Can. J. Chem.* **2009**, *87*, 790−797.
(35) Frisch, M. J.; Trucks, G. W.; Schlegel, H. B.; Scuseria, G. E.; Robb, M. A.; Cheeseman, J. R.; Scalmani, G.; Barone, V.; Mennucci, B.; Petersson, G. A.; et al. *Gaussian 09*, revision A.02; Gaussian, Inc.: Wallingford, CT, 2009.
(36) Zhao, Y.; Truhlar, D. G. *Theor. Chem. Acc.* **2008**, *120*, 215−241.
(37) Marenich, A. V.; Cramer, C. J.; Truhlar, D. G. *J. Phys. Chem. B* **2009**, *113*, 6378−96.
(38) Ho, J.; Coote, M. L.; Franco-Pérez, M.; Gómez-Balderas, R. *J. Phys. Chem. A* **2010**, *114*, 11992−12003.
(39) Swart, M.; Rösler, E.; Bickelhaupt, F. M. *J. Comput. Chem.* **2006**, *27*, 1486−1493.
(40) Kelly, C. P.; Cramer, C. J.; Truhlar, D. G. *J. Phys. Chem. B* **2006**, *110*, 16066−16081.
(41) Patungwasa, W.; Hodak, J. H. *Mater. Chem. Phys.* **2008**, *108*, 45−54.
(42) Silva, A. M. N.; Kong, X.; Hider, R. C. *Biometals* **2009**, *22*, 771−778.
(43) Soni, V.; Sindal, R. S.; Mehrotra, R. N. *Inorg. Chim. Acta* **2007**, *360*, 3141−3148.
(44) Wu, X.; Redmond, P. L.; Liu, H.; Chen, Y.; Steigerwald, M.; Brus, L. *J. Am. Chem. Soc.* **2008**, *130*, 9500−9506.
(45) The PyMOL Molecular Graphics System, Version 1.3 Schrödinger, LLC.
(46) Peck, J. A.; Tait, C. D.; Swanson, B. I.; Brown, G. E., Jr. *Geochim. Cosmochim. Acta* **1991**, *55*, 671−676.
(47) Basolo, F.; Pearson, R. G. In *Mechanism of Inorganic Reactions: a study of metal complexes in solution*; John Wiley: New York, 1958; p 384.
(48) Scott, V. J.; Labinger, J. A.; Bercaw, J. E. *Organometallics* **2010**, *29*, 4090−4096.
(49) Soni, V.; Sindal, R. S.; Mehrotra, R. N. *Polyhedron* **2005**, *24*, 1167−1174.

(50) Berglund, J.; Elding, L. I. *Inorg. Chem.* **1995**, *34*, 513−519.

(51) Doskocz, M.; Roszak, S.; Majumdar, D.; Doskocz, J.; Gancarz, R.; Leszczynski, J. *J. Phys. Chem. A* **2008**, *112*, 2077−2081.

(52) Xie, H.; Xia, F.; Cao, Z. *J. Phys. Chem. A* **2007**, *111*, 4384−4390.

(53) Casado, R.; Contel, M.; Laguna, M.; Romero, P.; Sanz, S. *J. Am. Chem. Soc.* **2003**, *125*, 11925−11935.

(54) Fackler, J. P., Jr.; Khan, M. N. I.; King, C.; Staples, R. J.; Winpenny, R. E. P. *Organometallics* **1991**, *10*, 2178−2183.

23691

dx.doi.org/10.1021/jp305830p | *J. Phys. Chem. C* 2012, 116, 23682−23691